

# Lawrence Berkeley National Laboratory

LBL Publications

## Title

Probing molecular bond-length using molecular-frame photoelectron angular distributions

## Permalink

<https://escholarship.org/uc/item/5js7b4n9>

## Journal

The Journal of Chemical Physics, 150(17)

## ISSN

0021-9606

## Authors

Fukuzawa, Hironobu

Lucchese, Robert R

Liu, Xiao-Jing

et al.

## Publication Date

2019-05-07

## DOI

10.1063/1.5091946

Peer reviewed

# Probing molecular bond-length using molecular-frame photoelectron angular distributions

Hironobu Fukuzawa,<sup>1, a)</sup> Robert R. Lucchese,<sup>1, 2, b)</sup> Xiao-Jing Liu,<sup>1, c)</sup> Kentaro Sakai,<sup>1</sup> Hiroshi Iwayama,<sup>3, d)</sup> Kiyonobu Nagaya,<sup>3</sup> Katharina Kreidi,<sup>4</sup> Markus S. Schöffler,<sup>4</sup> James R. Harries,<sup>5, e)</sup> Yusuke Tamenori,<sup>5</sup> Yuichiro Morishita,<sup>6</sup> Isao H. Suzuki,<sup>6, 7</sup> Norio Saito,<sup>6</sup> and Kiyoshi Ueda<sup>1, f)</sup>

<sup>1)</sup>*Institute of Multidisciplinary Research for Advanced Materials, Tohoku University, Sendai 980-8577, Japan*

<sup>2)</sup>*Chemical Sciences Division, Lawrence Berkeley National Laboratory, Berkeley CA 94720, USA*

<sup>3)</sup>*Department of Physics, Kyoto University, Kyoto 606-8502, Japan*

<sup>4)</sup>*Goeth-Universität Frankfurt am Main, Max-von-Laue-Str 1, D-60438 Frankfurt, Germany*

<sup>5)</sup>*Japan Synchrotron Radiation Research Institute, Sayo, Hyogo 679-5198, Japan*

<sup>6)</sup>*National Metrology Institute of Japan, AIST, Tsukuba 305-8568, Japan*

<sup>7)</sup>*Photon Factory, Institute of Material Structure Science, Tsukuba 305-0801, Japan*

(Dated: 8 April 2019)

The molecular-frame photoelectron angular distributions (MFPADs) in O 1s photoemission from CO<sub>2</sub> molecule were measured. Patterns due to photoelectron diffractions were observed in the MFPADs. The polarization-averaged MFPADs were compared with theoretical calculation and were found to be useful in determining the molecular bond-length, which is a component to determine molecular structures.

## I. INTRODUCTION

Probing molecular structures during reactions, i.e. creating a “molecular movie”, is key to understanding and ultimately controlling such reactions. In order to capture ultrafast reactions progressing in the femtosecond scale, we must obtain a tool for such “movie” creation which also has femtosecond resolution. The advent of intense optical lasers and free-electron lasers enable us to initiate ultrafast reactions with femtosecond control. The missing step is also to use such time resolved lasers to extract the instantaneous structure of a molecule during the course of the reaction.

X-ray diffraction (XRD)<sup>1</sup> and electron diffraction (ED)<sup>2</sup> are well established techniques for probing the structure of matter, in particular, the positions of atoms inside a molecule. These methods are based on high energy x-rays or high energy electrons. High energies are desirable since the de Broglie wavelength is small, which is essential for achieving high spatial resolution, additionally at high energies the scattering is simple so that extracting structure information from diffraction data is relatively easy. However, at high energies scattering cross sections are small. Thus XRD is often carried out with condensed phase samples. High energy ED can be applied to gas phase molecules due to strong interaction of changed particles with matter.<sup>3</sup> Recent developments of ultrafast x-ray and electron sources has opened up new possibilities of extend-

ing the structure determination to the femtosecond timescale at which the dynamics, e.g. atomic motion and structural changes, occur (see, e.g. a recent review by R.J.D. Miller<sup>4</sup>). Probing structural changes in gas phase molecules at the femtosecond timescale by ED<sup>5</sup> and XDR<sup>6</sup> is, however, still challenging today.

The ED described above employs external electron sources. An alternative approach is to use electrons emitted from within the sample. Well-known extended x-ray absorption fine structure (EXAFS) spectroscopy is a technique based on the “from within” concept, which probes the local structure close to the site where the core-level photoelectron is emitted. Another “from within” technique used for probing, e.g., surface structure, is photoelectron diffraction (PED) where the directions of the photoemission are measured relative to the sample orientation.<sup>7</sup> The feasibility of both EXAFS<sup>8,9</sup> and PED<sup>10</sup> has been demonstrated also for gas-phase molecules using synchrotron radiation sources. Compared to the standard ED and XRD, the retrieval of molecular structure relies on more sophisticated theories. Although applying PED to femtosecond time-resolved study of gas-phase molecules using X-ray free-electron lasers has been proposed<sup>11</sup> and indeed there are some attempts towards this direction with newly emerging short wavelength free-electron lasers,<sup>12–15</sup> there has been no report on time-resolved studies so far. Other approaches using laboratory lasers such as laser-assisted electron diffraction<sup>16</sup>, and laser-induced electron diffraction<sup>17–20</sup>, have been proposed and developments are in progress.

In this study, we probe one of the components of the molecular structure, bond-length, using molecular-frame photoelectron angular distributions (MFPADs). Williams *et al.* measured three dimensional MFPADs in the C 1s photoemission from CH<sub>4</sub> molecule and found that the polarization-averaged MFPADs (PA-MFPAD) reflect bond directions of the molecule<sup>21</sup>. Here we use a linear molecule, CO<sub>2</sub> as a target molecule and focus on the dependence of the PA-MFPAD on the bond-length.

<sup>a)</sup>Electronic mail: fukuzawa@tohoku.ac.jp

<sup>b)</sup>Electronic mail: rlucchese@lbl.gov

<sup>c)</sup>Current address: School of Physical Science and Technology, ShanghaiTech University, Shanghai 201210, China.

<sup>d)</sup>Current address: UVSOR Facility, Institute of Molecular Science, Okazaki 444-8585, Japan.

<sup>e)</sup>Current address: QST, SPring-8, Kouto 1-1-1, Sayo, Hyogo 679-5148, Japan.

<sup>f)</sup>Electronic mail: kiyoshi.ueda@tohoku.ac.jp

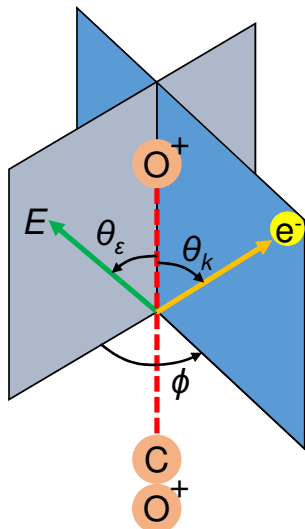


FIG. 1. The molecular frame. The molecular axis (dashed line) is determined by the release directions of  $O^+$  and  $CO^+$ .  $\theta_k$  is the angle between the electron momentum vector and the molecular axis.  $\theta_\epsilon$  is angle between the electric vector of the incident light and the molecular axis. Two planes are shown in the figure. One contains the electron emission direction vector and the molecular axis. The other contains the electric vector and the molecular axis.  $\phi$  corresponds to angle between two planes.

## II. METHODS

### A. Experimental method

The experiment has been carried out at the c-branch of the beam line BL27SU of SPring-8<sup>22–24</sup>, using the 26 single-bunches + 2/29 filling mode, which provides a single-bunch separation of 165.2 ns. Linearly polarized incident light crosses with supersonic  $CO_2$  jet at a right angle.

Our experimental method is based on the coincidence measurement of electron and ion times of flight (TOFs) using two multihit two-dimensional position sensitive detectors, and is equivalent to cold-target recoil momentum spectroscopy or the reaction microscope<sup>25–27</sup>. The TOF axis is perpendicular to both the gas and photon beams. Ions are accelerated by a uniform electrostatic field to a detector at one end of the acceleration region while the same field accelerates electrons in the opposite direction where they enter a drift region. Each detector is fitted with a two-dimensional (2D) multihit readout delay-line anode (Roentdek)<sup>28</sup>. This permits measurements of the TOF and 2D detection position coordinates, thus allowing us to extract the three-dimensional (3D) momentum. The orientation of the molecular axis at the time of photoemission is extracted from the momentum vectors of the  $O^+$  and  $CO^+$  fragments resulting from Coulomb dissociation of  $CO^{2+}$  formed via rapid Auger decay, within the axial-recoil approximation<sup>29</sup>. Figure 1 illustrates the molecular frame.

### B. Theoretical method

To extract structural parameters from the measured PA-MFPADs, we computed the PA-MFPADs as a function of molecular geometry, indicated by the variable  $q$ , and performed a least-squares fit of computed PA-MFPADs and experimental PA-MFPADs with respect to variations in  $q$  in the computation.

The fixed-geometry MFPAD intensity, from which the PA-MFPADs are derived, can be written in terms of the  $F_{LN}$  functions as<sup>30</sup>

$$I(\theta_k, \phi, \theta_\epsilon, q) = F_{00}(\theta_k, q) + F_{20}(\theta_k, q) P_2^0(\cos \theta_\epsilon) + F_{21}(\theta_k, q) P_2^1(\cos \theta_\epsilon) \cos(\phi) + F_{22}(\theta_k, q) P_2^2(\cos \theta_\epsilon) \cos(2\phi) \quad (1)$$

using the coordinated system indicated in Figure 1, where  $\phi = \theta_k - \theta_\epsilon$ . The explicit expressions for obtaining the MFPADs from computed dipole transition matrix elements are given in the supplementary material. A dimensionless form of the  $F_{LN}$  functions can be written as<sup>31</sup>

$$\bar{F}_{LN}(\theta_k, q) = \frac{4\pi}{\sigma(q)} F_{LN}(\theta_k, q) \quad (2)$$

where the total cross section as a function of geometry,  $\sigma(q)$ , can be obtained from  $F_{00}$  using

$$\sigma(q) = 2\pi \int_0^\pi F_{00}(\theta_k, q) \sin \theta_k d\theta_k. \quad (3)$$

To obtain the PA-MFPAD we average the MFPAD with respect to polarization direction which is obtained by integrating Eq. (1) over  $\phi$  and  $\theta_\epsilon$  and dividing by  $4\pi$ . The dimensionless PA-MFPAD is then

$$\bar{I}^{PA}(\theta_k, q) = \bar{F}_{00}(\theta_k, q). \quad (4)$$

The computed PA-MFPADs were obtained from fixed-nuclei transition matrix elements that were calculated using the multichannel Schwinger configuration interaction (MC-SCI) method<sup>32,33</sup>. The computed photoionization matrix elements were very similar to those found in Ref.<sup>34</sup>. The initial state and final ionic states were represented as configuration interaction (CI) wave functions. A series of PA-MFPADs were computed at different symmetric geometries with  $R(CO_1) = R(CO_2)$  near the the experimental  $r_0$  geometry of  $R(CO_1) = R(CO_2) = 1.1621 \text{ \AA}$ <sup>35</sup>. The one-electron basis set used to construct these bound state wave functions was the augmented correlation-consistent polarized valence triple-zeta (aug-cc-pVTZ) basis set of Dunning and coworkers<sup>36,37</sup>. The bound orbitals used in both the initial and final states were computed using a valence complete active space self-consistent field (VCASSCF) calculation on the initial ground state of the molecule. All bound state calculations were performed using the MOLPRO quantum chemistry code<sup>38</sup>.

In the MCSCI calculations of the fixed-nuclei transition matrix elements, the CI wave functions for both the initial and final ion states were obtained using the set of natural orbitals

obtained from the initial state VCASSCF. In the initial state, used in the MCSCI calculations, we included configuration state functions (CSFs) with up to three electrons in the three weakly-occupied natural-orbital shells, which were composed of two  $\sigma$  orbitals and one pair of  $\pi$  orbitals. In the ion states, only up to double excitations into the weakly occupied shells were considered. In these calculations, all electrons were active leading to 2709 CSFs for the initial state and 2391 CSFs for the ion states. In the ion state CI, the two core hole states were found to be eigenstate 601 in  $^2\Sigma_u^+$  symmetry and 602 in  $^2\Sigma_g^+$  symmetry. In all scattering calculations we included two ionization channels corresponding to the two O 1s core hole states. All integrals were performed using a single-center expansion (SCE) including partial waves up to  $l_{\max} = 80$ .

### III. RESULTS AND DISCUSSION

In order to extract the MFPADs from the experimental data, we have employed the projection method<sup>31,39</sup>. Our projection method uses the fact that the expansion in Eq. (1) is written in terms of orthogonal polynomials of  $\theta_\epsilon$  and  $\phi$  such that the  $F_{JN}(\theta_k)$  can be obtained using

$$F_{JN}(\theta_k) = \frac{(2J+1)(J-N)!}{2\pi(1+\delta_{N,0})(J+N)!} \int_0^\pi \sin\theta_k d\theta_k \times \int_0^{2\pi} d\phi I(\theta_k, \phi, \theta_\epsilon) P_J^N(\cos\theta_\epsilon) \cos(N\phi). \quad (5)$$

In this method, all possible experimental information is encapsulated in the four one-dimensional  $F_{JN}$  functions. The measurements are on a relative scale and thus the  $F_{JN}$  functions are only relative. **The  $F_{JN}$  functions obtained from the experiment are shown in the supplementary material.**

Using the obtained  $F_{JN}$  functions, we can reconstruct MFPADs for any angle  $\theta_\epsilon$  between the molecular axis and the  $E$  vector<sup>40</sup>. Figure 2 shows the MFPAD in the plane defined by the  $E$  vector of the incident light and the molecular axis, i.e.,  $\phi = 0$ . There are several islands of high intensity and their positions change with the photon energy, i.e. the photoelectron energy change. In the O 1s photoemissions, the electron emission direction is dominated by stripes along the  $\theta_k = \theta_\epsilon$  diagonal seen in Figure 2, as would be expected from photoemission from an isolated  $s$  state. However, in the emission from the O 1s in CO<sub>2</sub> we see that there is additionally structure that appears as the islands of enhanced intensity along the diagonals. This additional structure is due to photoelectron diffraction by the other atoms in the molecule, i.e. the carbon atom and the second oxygen atom. Thus, pattern of the islands along the diagonal has information about the distances between carbon and oxygen atoms in CO<sub>2</sub>.

The above described structural information can also be captured in the PA-MFPAD rather than the polarization dependent MFPAD. Thus in the next step, we construct the PA-MFPADs. The patterns shown in Figure 2 are asymmetric. The asymmetry is due to core-hole localization in O 1s ionization of CO<sub>2</sub>. By selecting different kinetic energy releases of the fragment ions, it may be possible to separate the symmetric pattern and the asymmetric pattern due to core-hole

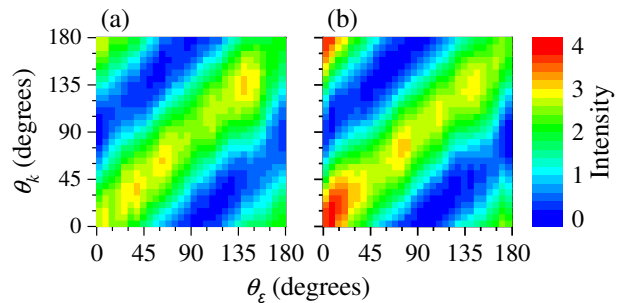


FIG. 2. The MFPADs for O 1s electron emission from CO<sub>2</sub> in the plane spanned by the  $E$  vector of the incident light and the molecular axis. The photon energies are 569.25 eV (a) and 574.75 eV (b).

localization and delocalization, respectively<sup>41</sup>. Since the degree of localization is only determined by the Auger decay and subsequent dissociation dynamics of the CO<sub>2</sub><sup>+</sup> 1s hole states, we can determine the bond-length **at the time of photoionization** by including both the contributions from the localized or delocalized core-holes. To remove the effects of localization, we symmetrize  $F_{00}(\theta_k)$  obtained from the projection analysis and use the symmetrized function in the PA-MFPAD in the following discussion.

Figure 3 depicts the experimental and theoretical PA-MFPADs for the O 1s photoemission at the photon energies of 569.25 eV and 574.75 eV. The theoretical fixed-nuclei PA-MFPADs were calculated at C–O bond-lengths which varied from 1.087 Å to 1.237 Å, i.e. from  $-0.075$  Å to  $+0.075$  Å relative to the **experimental  $r_0$**  distance (1.1621 Å<sup>35</sup>) of the CO<sub>2</sub> molecule in the ground state. The theoretical PA-MFPADs were convoluted with a Gaussian with 21 degrees fwhm in order to compare with the experimental data. The shape of the PA-MFPAD changes when the bond-length is changed, and thus the PA-MFPAD is seen to be sensitive to the bond-length.

It should be noted that the theoretical calculations employed here include the full electron-molecular ion scattering dynamics and thus we can accurately treat relatively low kinetic energies such as 28.0 eV and 33.5 eV considered here, which occur at photon energies 569.25 eV and 574.75 eV. At such low energies, simple models commonly employed to model photoelectron scattering<sup>10,11,14,15</sup> may fail. Comparison between the experimental and theoretical results gives us the **average value of the C–O bond length** when the O 1s photoemission occurs. We obtained bond-lengths  $1.19 \pm 0.05$  Å and  $1.16 \pm 0.05$  Å for 569.25 eV and 574.75 eV photon energies, respectively, **by a root mean square analysis using weights obtained from the experimental errors.** The bond-length obtained from different photon energies reasonably agree with each other and with **the  $r_g$  bond length of CO<sub>2</sub> molecule in the ground state (1.1653 Å<sup>42</sup>)**. Thus, the PA-MFPAD is useful for determining the bond-length.

In summary, we have measured the PA-MAPADs for the O 1s photoemission from CO<sub>2</sub> molecule using electron-ion coincidence spectroscopy and demonstrated that the PA-MAPADs are sensitive to changes in the molecular geometry. This method has the potential to be a tool for making “molec-

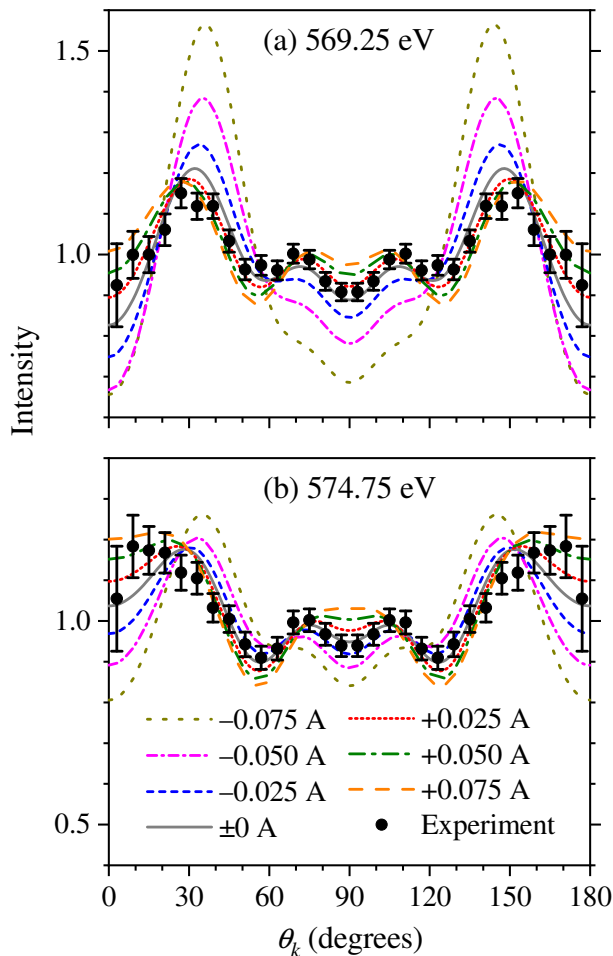


FIG. 3. The PA-MFPADs of CO<sub>2</sub> at the photon energies of (a) 569.25 eV and (b) 574.75 eV. Lines in different colors indicate calculated results using different C–O bond-length with respect to the equilibrium internuclear distance of neutral CO<sub>2</sub> in the ground state. Embedded circles with error bar indicate the experimental results.

ular movies” on the femtosecond time scale by using high-energy short-pulse light sources such as free-electron lasers.

### SUPPLEMENTARY MATERIAL

The supplementary material gives the detailed formulas connecting computed dipole matrix elements and the MFPAD. Additionally the supplementary material contains a plot of the four experimental  $F_{JN}$  functions for both 569.25 eV and 574.75 eV photon energies.

### ACKNOWLEDGMENTS

The experiments were performed at the BL27SU of SPring-8 with the approval of the Japan Synchrotron Radiation Research Institute (JASRI) (Proposal No. 2007A1394 and

2007A1602). This study was supported by the X-ray Free Electron Laser Priority Strategy Program of the Ministry of Education, Culture, Sports, Science and Technology of Japan (MEXT), by the Japan Society for the Promotion of Science (JSPS) KAKENHI Grant Number 15K17487, by Dynamic Alliance for Open Innovation Bridging Human, Environment and Materials, by the Research Program of “Dynamic Alliance for Open Innovation Bridging Human, Environment and Materials” in “Network Joint Research Center for Materials and Devices”, and by IMRAM project. The theoretical work was performed at LBNL under the auspices of the US DOE under Contract DE-AC02-05CH11231 and was supported by the US DOE Office of Basic Energy Sciences, Chemical Sciences, Geosciences, and Biosciences Division.

<sup>1</sup>E. O. Wollan, Rev. Mod. Phys. **4**, 205 (1932).

<sup>2</sup>L. O. Brockway, Rev. Mod. Phys. **8**, 231 (1936).

<sup>3</sup>I. Hargittai, *Gas-phase Electron Diffraction for Molecular Structure Determination*, in *Electron Crystallography NATO Science Series II: Mathematics, Physics and Chemistry*, edited by T. E. Weirich, J. L. Lábár, and X. Zou (Springer, Dordrecht, 2006) Vol. 211, pp 197–206.

<sup>4</sup>R. J. D. Miller, Science **343**, 1108 (2014).

<sup>5</sup>A. H. Zweil, *4D Visualization of Matter: Recent Collected Works* (Imperial College Press, London, 2008).

<sup>6</sup>M. P. Minitti, J. M. Budarz, A. Kirrander, J. S. Robinson, D. Ratner, T. J. Lane, D. Zhu, J. M. Glowina, M. Kozina, H. T. Lemke, M. Sikorski, Y. Feng, S. Nelson, K. Saita, B. Stankus, T. Northey, J. B. Hastings, and P. M. Weber, Phys. Rev. Lett. **114**, 255501 (2015).

<sup>7</sup>D. P. Woodruff, Appl. Phys. A **92**, 439 (2008).

<sup>8</sup>K. Ueda, C. Miron, E. Plésiat, L. Argenti, M. Patanen, K. Kooser, D. Ayuso, S. Mondal, M. Kimura, K. Sakai, O. Travnikova, A. Palacios, P. Decleva, E. Kukuk, and F. Martín, J. Chem. Phys. **139**, 124306 (2013).

<sup>9</sup>E. Kukuk, D. Ayuso, T. D. Thomas, P. Decleva, M. Patanen, L. Argenti, E. Plésiat, A. Palacios, K. Kooser, O. Travnikova, S. Mondal, M. Kimura, K. Sakai, C. Moron, F. Martín, and K. Ueda, Phys. Rev. A **88**, 033412 (2013).

<sup>10</sup>M. Kazama, T. Fujikawa, N. Kishimoto, T. Mizuno, J. Adachi, and A. Yagishita, Phys. Rev. A **87**, 063417 (2013).

<sup>11</sup>F. Krasniqi, B. Najjari, L. Strüder, D. Rolles, A. Voitkiv, and J. Ullrich, Phys. Rev. A **81**, 033411 (2010).

<sup>12</sup>A. Rouzée, P. Johnsson, L. Rading, A. Hundertmark, W. Siu, Y. Huismans, S. Düsterer, H. Redlin, F. Tavella, N. Stojanovic, A. Al-Shemmary, F. Lépine, D. M. P. Holland, T. Schlatholter, R. Hoekstra, H. Fukuzawa, K. Ueda, and M. J. J. Vrakking, J. Phys. B: At. Mol. Opt. Phys. **46**, 164029 (2013).

<sup>13</sup>R. Boll, D. Anielski, C. Bostedt, J. D. Bozek, L. Christensen, R. Coffee, S. De, P. Decleva, S. W. Epp, B. Erk, L. Foucar, F. Krasniqi, J. Küpper, A. Rouzée, B. Rudek, A. Rudenko, S. Schorb, H. Stapelfeldt, M. Stener, S. Stern, S. Techert, S. Trippel, M. J. J. Vrakking, J. Ullrich, and D. Rolles, Phys. Rev. A **88**, 061402 (2013).

<sup>14</sup>K. Nakajima, T. Teramoto, H. Akagi, T. Fujikawa, T. Majima, S. Minemoto, K. Ogawa, H. Sakai, T. Togashi, K. Tono, S. Tsuru, K. Wada, M. Yabashi, and A. Yagishita, Sci. Rep **5**, 14065 (2015).

<sup>15</sup>S. Minemoto, T. Teramoto, H. Akagi, T. Fujikawa, T. Majima, K. Nakajima, K. Niki, S. Owada, H. Sakai, T. Togashi, K. Tono, S. Tsuru, K. Wada, M. Yabashi, S. Yoshida, and A. Yagishita, Sci. Rep **6**, 38654 (2016).

<sup>16</sup>Y. Morimoto, R. Kanya, and K. Yamanouchi, J. Chem. Phys. **140**, 064201 (2014).

<sup>17</sup>J. Xu, Z. Chen, A.-T. Le, and C. D. Lin, Phys. Rev. A **82**, 033403 (2010).

<sup>18</sup>C. I. Blaga, J. Xu, A. D. DiChiara, E. Sistrunk, K. Zhang, P. Agostini, T. A. Miller, L. F. DiMauro, and C. D. Lin, Nature **483**, 194 (2012).

<sup>19</sup>M. G. Pullen, B. Wolter, A.-T. Le, M. Baudisch, M. Hemmer, A. Senftleben, C. D. Schröter, J. Ullrich, R. Moshhammer, C. D. Lin, and J. Biegert, Nat. Commun. **6**, 7262 (2015).

<sup>20</sup>Y. Ito, C. Wang, A.-T. Le, M. Okunishi, D. Ding, C. D. Lin, and K. Ueda, Struct. Dyn. **3**, 034303 (2016).

<sup>21</sup>J. B. Williams, C. S. Trevisan, M. S. Schöffler, T. Jahnke, I. Bocharova, H. Kim, B. Ulrich, R. Wallauer, F. Sturm, T. N. Rescigno, A. Belkacem, R.

- Dörner, Th. Weber, C. W. McCurdy, and A. L. Landers, *Phys. Rev. Lett.* **108**, 233002 (2012).
- <sup>22</sup>H. Ohashi, E. Ishiguro, Y. Tamenori, H. Kishimoto, M. Tanaka, M. Irie, T. Tanaka, and T. Ishikawa, *Nucl. Instrum. Methods A* **467–468**, 529 (2001).
- <sup>23</sup>H. Ohashi, E. Ishiguro, Y. Tamenori, H. Okumura, A. Hiraya, H. Yoshida, Y. Senba, K. Okada, N. Saito, I. H. Suzuki, K. Ueda, T. Ibuki, S. Nagaoka, I. Koyano, and T. Ishikawa, *Nucl. Instrum. Methods A* **467–468**, 533 (2001).
- <sup>24</sup>K. Ueda, *J. Phys. B: At. Mol. Opt. Phys.* **36**, R1 (2003).
- <sup>25</sup>R. Dörner, V. Mergel, O. Jagutzki, L. Spielberger, J. Ullrich, R. Moshhammer, H. Schmidt-Böcking, *Phys. Rep.* **330**, 95 (2000).
- <sup>26</sup>J. Ullrich, R. Moshhammer, A. Dorn, R. Dörner, L. Ph. H. Schmidt, H. Schmidt-Böcking, *Rep. Prog. Phys.* **66**, 1463 (2003).
- <sup>27</sup>K. Ueda, H. Fukuzawa, X.-J. Liu, K. Sakai, G. Prümper, Y. Morishita, N. Saito, I. H. Suzuki, K. Nagaya, H. Iwayama, M. Yao, K. Kreidi, M. Schöffler, T. Jahnke, S. Schössler, R. Dörner, Th. Weber, J. Harries, and Y. Tamenori, *J. Electron Spectrosc. Relat. Phenom.* **166–167**, 3 (2008).
- <sup>28</sup>O. Jagutzki, A. Cerezo, A. Czasch, R. Dörner, M. Hattabaß, M. Huang, V. Mergel, U. Spillmann, K. Ullmann-Pfefer, T. Weber, H. Schmidt-Böcking, and G. D. W. Smith, *IEEE Trans. Nucl. Sci.* **49**, 2477 (2002).
- <sup>29</sup>R. N. Zare, *Mol. Photochem.* **4**, 1 (1972).
- <sup>30</sup>A. Lafosse, J. C. Brenot, P. M. Guyon, J. C. Houver, A. V. Golovin, M. Lebech, D. Dowek, P. Lin, and R. R. Lucchese, *J. Chem. Phys.* **117**, 8368 (2002).
- <sup>31</sup>X.-J. Liu, R. R. Lucchese, A. N. Grum-Grzhimailo, Y. Morishita, N. Saito, G. Prümper, and K. Ueda, *J. Phys. B: At. Mol. Opt. Phys.* **40**, 485 (2007).
- <sup>32</sup>R. E. Stratmann and R. R. Lucchese, *J. Chem. Phys.* **102**, 8493 (1995).
- <sup>33</sup>R. E. Stratmann, R. W. Zurales, and R. R. Lucchese, *J. Chem. Phys.* **104**, 8989 (1996).
- <sup>34</sup>R. R. Lucchese, H. Fukuzawa, X.-J. Liu, T. Teranishi, N. Saito, and K. Ueda, *J. Phys. B: At. Mol. Opt. Phys.* **45**, 194014 (2012).
- <sup>35</sup>G. Herzberg, *Molecular Spectra and Electronic Structure: III. Electronic Spectra and Electronic Structure of Polyatomic Molecules* (Van Nostrand-Reinhold, New York, 1966).
- <sup>36</sup>T. H. Dunning, Jr. *J. Chem. Phys.* **90**, 1007 (1989).
- <sup>37</sup>R. A. Kendall, T. H. Dunning, Jr., and R. J. Harrison, *J. Chem. Phys.* **96**, 6796 (1992).
- <sup>38</sup>H.-J. Werner, P. J. Knowles, G. Knizia, F. R. Manby, M. Schütz, P. Celani, W. Györffy, D. Kats, T. Korona, R. Lindh, A. Mitrushenkov, G. Rauhut, K. R. Shamasundar, T. B. Adler, R. D. Amos, S. J. Bernhardsson, A. Berning, D. L. Cooper, M. J. O. Deegan, A. J. Dobbyn, F. Eckert, E. Goll, C. Hampel, A. Hesselmann, G. Hetzer, T. Hrenar, G. Jansen, C. Köppl, Y. Liu, A. W. Lloyd, R. A. Mata, A. J. May, S. J. McNicholas, W. Meyer, M. E. Mura, A. Nicklass, D. P. O’Neill, P. Palmieri, D. Peng, K. Pflüger, R. Pitzer, M. Reiher, T. Shiozaki, H. Stoll, A. J. Stone, R. Tarroni, T. Thorsteinsson, M. Wang, MOLPRO, version 2015.1, a package of ab initio programs, 2015.
- <sup>39</sup>R. R. Lucchese, R. Montuoro, A. N. Grum-Grzhimailo, X.-J. Liu, G. Prümper, Y. Morishita, N. Saito, and K. Ueda, *J. Electron Spectrosc. Relat. Phenom.* **155**, 95 (2007).
- <sup>40</sup>R. R. Lucchese, A. Lafosse, J. C. Brenot, P. M. Guyon, J. C. Houver, M. Lebech, G. Raseev, and D. Dowek, *Phys. Rev. A* **65**, 020702 (2002).
- <sup>41</sup>R. Guillemin, P. Declève, M. Stener, C. Bomme, T. Marin, L. Journel, T. Marchenko, R. K. Kushawaha, K. Jänkälä, N. Trcera, K. P. Bowen, D. W. Lindle, M. N. Piancastelli, and M. Simon, *Nat. Commun.* **6**, 6166 (2015).
- <sup>42</sup>M. Hargittai and I. Hargittai, *Int. J. Quantum Chem.* **44**, 1057 (1992).